

# Gamma: Toward Generic Image Assessment with Mixture of Assessment Experts

Hantao Zhou<sup>1</sup> Rui Yang<sup>2</sup> Longxiang Tang<sup>1</sup> Guanyi Qin<sup>3</sup> Yan Zhang<sup>4</sup> Runze Hu<sup>5</sup> Xiu Li<sup>1</sup>

## Abstract

Image assessment aims to evaluate the quality and aesthetics of images and has been applied across various scenarios, such as natural and AIGC scenes. Existing methods mostly address these sub-tasks or scenes individually. While some works attempt to develop unified image assessment models, they have struggled to achieve satisfactory performance or cover a broad spectrum of assessment scenarios. In this paper, we present **Gamma**, a **Generic imAge assessMent** model using **Mixture of Assessment Experts**, which can effectively assess images from diverse scenes through mixed-dataset training. Achieving unified training in image assessment presents significant challenges due to annotation biases across different datasets. To address this issue, we first propose a **Mixture of Assessment Experts (MoAE)** module, which employs shared and adaptive experts to dynamically learn common and specific knowledge for different datasets, respectively. In addition, we introduce a **Scene-based Differential Prompt (SDP)** strategy, which uses scene-specific prompts to provide prior knowledge and guidance during the learning process, further boosting adaptation for various scenes. Our **Gamma** model is trained and evaluated on 12 datasets spanning 6 image assessment scenarios. Extensive experiments show that our unified **Gamma** outperforms other state-of-the-art mixed-training methods by significant margins while covering more scenes.

## 1. Introduction

Image assessment is a long-standing research topic in the field of image processing, primarily comprising two tasks: Image Quality Assessment (IQA) and Image Aesthetic As-

\*Equal contribution <sup>1</sup>Tsinghua University <sup>2</sup>The University of Hong Kong <sup>3</sup>National University of Singapore <sup>4</sup>Xiamen University <sup>5</sup>Beijing Institute of Technology. Correspondence to: Xiu Li <li.xiu@sz.tsinghua.edu.cn>.

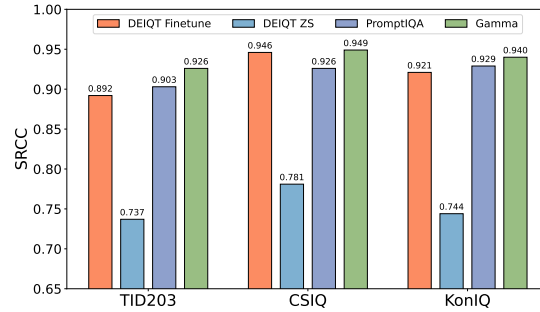


Figure 1. “DEIQT Finetune” is trained and tested on the same dataset. “DEIQT ZS” directly assesses images using the model trained on other datasets, which perform poorly. PromptIQA and our Gamma are trained on mixed datasets. Our Gamma performs well on multiple datasets simultaneously and even surpasses the task-specific method DETQT.

essment (IAA). These tasks require models to automatically evaluate the visual quality and aesthetic appeal of images, respectively. They have broad applications in various real-world scenarios, such as guiding image dehazing (Zhao et al., 2021), selecting high-quality images in a data engine (Rombach et al., 2022), serving as tools in an agentic system (Yang et al., 2024), or acting as reward models when aligning image generative models with human feedback (Liang et al., 2024).

Due to differences in image content and application scenarios, image assessment has spawned many sub-tasks, such as Natural-IQA for natural images, Face-IQA for facial images, AIGC-IQA for generated images, and IAA. Accordingly, numerous methods (Ke et al., 2021; He et al., 2022; Su et al., 2023b) have been proposed to address these specific tasks. However, these models often struggle to apply directly to other scenes or typically require task-specific fine-tuning on a given dataset. As illustrated in Figure 1, it is challenging for DEIQT (Qin et al., 2023) to transfer to other datasets without fine-tuning. This limitation prevents image assessment models from being widely applicable, e.g., IQA models are needed to assess facial, artistic, and natural images in the AIGC scene. Hence, there is an urgent need for a model that can effectively handle a variety of scenarios.

To mitigate this issue, some approaches attempt to com-

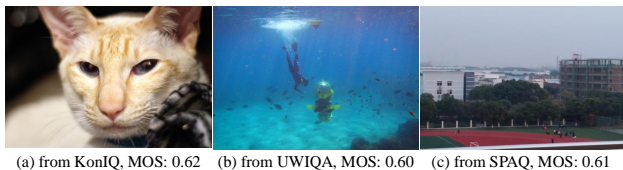


Figure 2. Images with similar MOS labels from different datasets exhibit drastically different perceptual quality. It is not hard to observe that image (a) has clearly superior quality than the other three. Zoom in for a better view.

bine many datasets from various assessment tasks to train a general image assessment model. For instance, UNIQUE (Zhang et al., 2021) and LIQE (Zhang et al., 2023) utilize multiple authentic and synthetic natural IQA datasets for mixed training, but they focus only on Natural-IQA. Q-Align (Wu et al., 2023) uses a large language model with billions of parameters to unify IQA and IAA tasks, but it has a low inference speed and focuses solely on natural images. Additionally, PromptIQA (Chen et al., 2024b) employs image-score pairs as prompts for quality predictions, but it is inflexible as it requires multiple images as references during inference. These methods, however, fail to achieve competitive performance compared to models trained on specific datasets and cover a broad range of scenes. Thus, it is imperative to develop a foundational image assessment model capable of evaluating images from various scenes.

To this end, we present **Gamma**, a **Generic imAge assessMent** model using **Mixture of Assessment experts**, to achieve unified image assessment across multiple datasets effectively. We found that the primary challenge in mixed-dataset training is *the mean opinion score (MOS) bias* between different datasets, *e.g.*, images with similar MOS may exhibit different perceptual qualities across various datasets. As shown in Figure 2, samples from KonIQ (Hosu et al., 2020), UWIIQA (Yang et al., 2021a), and SPAQ (Fang et al., 2020) show obvious differences in perceptual quality despite being labeled with similar MOS. To address this challenge, we introduce a novel **Mixture of Assessment Experts (MoAE)** module in our Gamma model. MoAE consists of two types of experts: shared experts and adaptive experts. The shared experts are employed throughout to learn dataset-shared knowledge, while the adaptive experts are dynamically activated to varying degrees to learn dataset-specific knowledge. Additionally, an image-based router modulates the contributions of each adaptive expert. This strategy allows the model to capture common features while flexibly adjusting representative features for different datasets. Compared with general Mixture of Experts (MoE) (Shazeer et al., 2017) and Lora-based MoE (Liu et al., 2024), we equip the MoAE module only in the rear blocks instead of all blocks, making it more efficient. Secondly, we propose a **Scene-based Differential Prompt (SDP)**, which uses different prompts for different datasets accord-

ing to their scenes. This strategy provides scene-specific knowledge for representation learning of different datasets, guiding the mixed-dataset training process.

Our Gamma model is uniformly trained on a mixture of 12 datasets from 6 image assessment scenarios spanning IQA and IAA tasks. We then evaluate it on 12 datasets, demonstrating that it not only outperforms state-of-the-art (SOTA) mixed-training methods by notable margins, but also covers more scenarios. In some benchmarks, Gamma even surpasses some SOTA task-specific methods. Additionally, if we fine-tune our MoAE-equipped Gamma on specific datasets, it can achieve SOTA performance on 12 datasets. Moreover, the unified pre-trained Gamma can be utilized as a foundational model to significantly enhance other image assessment tasks, *e.g.*, medical image quality assessment, and can achieve SOTA performance after task-specific training. In summary, our contributions are:

- We present **Gamma**, a powerful and generic image assessment model, capable of accurately assessing images from various scenarios through mixed training.
- We propose a novel Mixture of Assessment Experts (MoAE) module to extract representative features adaptively and a Scene-based Differential Prompt (SDP) strategy to provide guidance for representation learning, thereby achieving effective mixed-dataset training.
- Extensive experiments show that Gamma achieves SOTA performance on 12 datasets across 6 image assessment scenes in both mixed training and task-specific training settings.

## 2. Related Work

### 2.1. Image Assessment

Image Assessment mainly includes two subtasks: Image Quality Assessment (IQA) and Image Aesthetic Assessment (IAA). In the deep learning era, these two tasks have achieved significant breakthroughs. For the IQA task, researchers develop various advanced techniques to improve performance, including multi-level feature aggregation (Li et al., 2018; Chen et al., 2024a; Xu et al., 2024; Zhang et al., 2018; Mittal et al., 2012b; Ying et al., 2020), adaptive convolution (Su et al., 2020), transformer methods (Ke et al., 2021; Qin et al., 2023), vision-language models (VLMs) (Wang et al., 2023; Zhang et al., 2023) and large language models (LLM) (You et al., 2023). Moreover, besides the natural image assessment, these are various IQA methods for other scenes, such as face IQA (Ou et al., 2021; Su et al., 2023b; Jo et al., 2023), AIGC IQA (Yuan et al., 2023), underwater IQA (Yang et al., 2021b; Guo et al., 2023; Yang & Sowmya, 2015; Liu et al., 2023). For the IAA task, numerous methods have also been proposed to improve performance, including

loss function (Talebi & Milanfar, 2018), novel transformer architecture (Tu et al., 2022), multi-level features (Hosu et al., 2019), theme information (He et al., 2022; Li et al., 2023b) and multimodal pre-training (Ke et al., 2023).

## 2.2. Mixed Training for Image Assessment

As a fundamental image processing task, image assessment has been effectively applied to various scenarios. Recently, some works have attempted to develop unified methods that can be used in multiple IQA settings through mixed-dataset training. UNIQUE (Zhang et al., 2021) sampled pairs of images from IQA datasets and computes the probability that the first image of each pair is of higher quality. StairIQA (Sun et al., 2023) designed separate IQA regression heads for each dataset. PromptIQA (Chen et al., 2024b) utilized a short sequence of Image-Score Pairs as prompts for quality predictions. Q-Align (Wu et al., 2023) used large language model (LLM) to unify IQA and IAA tasks. However, most existing works fail to achieve competitive performance with task-specific methods and do not cover various scenes. Our Gamma outperforms other SOTA mixed-training methods by significant margins while covering more scenes.

## 2.3. Mixture of Experts

Mixture-of-Experts (MoE) divides specific parts of the parameters into several subsets, each of which is called an expert. It sets up a router that assigns experts to different inputs. Recently, the MoE structure has achieved remarkable success in large language models (LLM). For instance, DeepSeekMoE (Dai et al., 2024) proposes a novel MoE architecture that uses shared and routed experts to extract common and dynamic knowledge simultaneously. Beyond the natural language processing tasks, the idea of MoE has also been applied to vision models (Dai et al., 2021; Riquelme et al., 2021; Chen et al., 2023) and multimodal transformers (Wang et al., 2022; Feng et al., 2023). In Gamma, we utilize novel MoE module to effectively learn specific and general features of multi-dataset.

# 3. Method

## 3.1. Preliminary

As a foundational vision-language model (VLM), CLIP (Radford et al., 2021) has shown significant promise in supporting a wide array of vision tasks. Specifically, CLIP is composed of a transformer-based visual encoder  $\mathcal{V}$  and a text encoder  $\mathcal{T}$ , which generate aligned visual representations  $I$  and text representations  $T$  for each image-text pair. Utilizing these features, we can compute cosine similarity scores between image and text pairs across different domains or tasks to perform task-specific

predictions, including image assessment tasks. Recently, to enhance CLIP’s capabilities in the field of image assessment, UniQA (Zhou et al., 2024b) fine-tuned CLIP on large-scale synthetic and authentic image-text datasets focused on image quality and aesthetics. This approach demonstrates excellent performance on both IQA and IAA tasks after task-specific fine-tuning. However, the model lacks foundational applicability across various image assessment scenarios without fine-tuning. Building on the unified training pipeline proposed in UniQA, we propose two approaches to confront MOS bias present in different datasets and develop a foundational image assessment model. In the following, we will provide a detailed exposition of its components.

## 3.2. Overview of Gamma

As illustrated in Figure 3, our Gamma employs a visual encoder  $\mathcal{V}$  to extract visual features  $I \in \mathbb{R}^d$ , and a text encoder  $\mathcal{T}$  to extract text features  $T \in \mathbb{R}^d$ . After these encoders, a tunable adapter is used to obtain a score  $q$  representing image quality or aesthetics, following the methods in (Zhang et al., 2023) and (Zhou et al., 2024b). This process can be described as:

$$q = \sum_{k=1}^5 C_k \text{Softmax}(I'^{\top} T_k / \tau), I' = \text{Adapter}(I), \quad (1)$$

where  $\{T_k\}_{k=1}^5 \in \mathbb{R}^{5 \times d}$  represents text features of five assessment-dependent text prompts, *e.g.*, {bad image, poor image, fair image, good image, perfect image}.  $\{C_k\}_{k=1}^5 \in \mathbb{R}^5$  is a learnable vector initialized to [0.2, 0.4, 0.6, 0.8, 1.0], and  $\tau$  is a temperature parameter. In practice, the Adapter( $\cdot$ ) consists of two fully connected layers with a ReLU( $\cdot$ ) activation function in between. Based on this structure, to confront MOS bias in the mixed dataset and effectively perform unified pre-training, we propose a **Mixture of Assessment Experts (MoAE)** module to adaptively learn dataset-shared and dataset-specific knowledge from different datasets. We just integrate the MoAE module into the last few layers of both encoders, as shown in Figure 3 (a). Notably, we only fine-tune the parameters of the MoAE modules for various tasks, keeping the other parameters frozen, which is a significant advantage of our method. Additionally, we introduce a **Scene-based Differential Prompt (SDP)**. It uses different prompts for datasets from different scenes, thereby providing useful scene-based guidance for mixed-dataset training.

## 3.3. Mixture of Assessment Experts

To develop a unified and generic image assessment model, we aim to combine multiple image assessment datasets for joint training. Unfortunately, the mean opinion score (MOS)

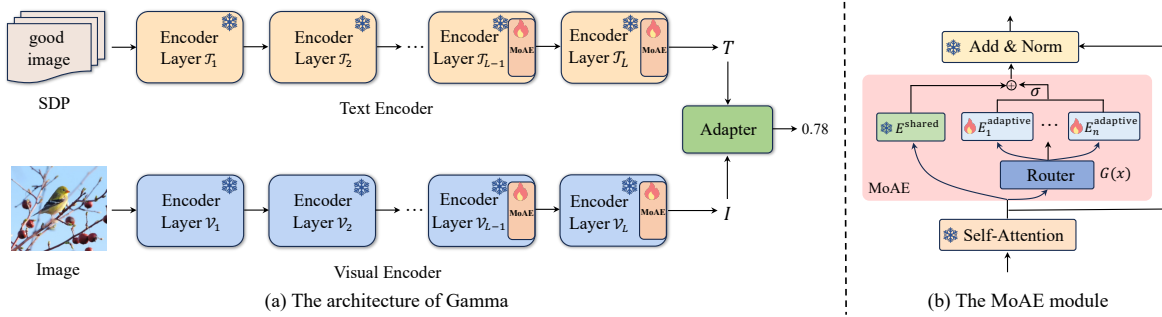


Figure 3. (a) The architecture of Gamma: It consists of a visual encoder  $\mathcal{V}$  and text encoder  $\mathcal{T}$ ; We add the Mixture of Assessment Experts (MoAE) to the last few layers of both encoders. We introduce a Scene-based Differential Prompt (SDP) to prompt images from different scenes (See Section 3.4 for details). (b) The MoAE module: It involves one shared expert ( $E^{\text{shared}}$ ) and several adaptive experts (from  $E_1^{\text{adaptive}}$  to  $E_n^{\text{adaptive}}$ ). We employ a router to adaptively activate the adaptive experts. We then use a learnable factor  $\sigma$  to merge the features of two type of experts.

introduces significant biases across different datasets, which hinders joint training. To address this challenge, we propose the MoAE module, where several experts are employed to learn the diverse biases of different datasets. As shown in Figure 3 (b), the proposed MoAE module includes a shared assessment expert ( $E^{\text{shared}}$ ) to learn common knowledge of image assessment and several adaptive assessment experts (from  $E_1^{\text{adaptive}}$  to  $E_n^{\text{adaptive}}$ ) to dynamically learn dataset-specific knowledge.

**The Shared Assessment Expert.** The shared assessment expert  $E^{\text{shared}}$  inherits the image assessment capabilities of the original CLIP model by reusing its weights. This expert remains frozen during training to ensure that the learned world knowledge is retained. Thus, the model can capture common representations across various contexts and maintain its original multi-modal capabilities. Given an input hidden state  $x \in \mathbb{R}^d$ , the output of the shared assessment expert is:

$$y^{\text{shared}} = E^{\text{shared}}(x), \quad (2)$$

where  $E^{\text{shared}}(\cdot)$  is implemented as the original feed-forward network (FFN) of the CLIP model.

**The Adaptive Assessment Expert.** The adaptive assessment expert module contains two components: (1)  $n$  experts  $\{E_i^{\text{adaptive}}\}_{i=1}^n$  to capture diverse facets of multi-dataset information; and (2) a router  $G(\cdot)$  to tailor the contribution of different experts based on the input feature. Given an input feature  $x \in \mathbb{R}^d$ , the output  $y^{\text{adaptive}}$  can be computed as:

$$y^{\text{adaptive}} = \sum_{i=1}^n G(x)_i E_i^{\text{adaptive}}(x), \quad (3)$$

$$G(x) = \text{Softmax}(Wx).$$

Here, the router  $G(\cdot)$  is a linear transformation for the input feature  $x$ ;  $W \in \mathbb{R}^{n \times d}$  is the transformation matrix. To avoid unreasonable weights, we utilize a Softmax operator to normalize the contribution weights. This ensures that the model

can learn dataset-specific knowledge efficiently. Notably, we initialize these experts with the weights of pre-trained CLIP to equip them with image assessment capabilities.

**MoAE Module.** Based on the above experts, the MoAE module merges the features of the two types of experts with a learnable factor  $\sigma$ , as shown on the right side of Figure 3. Thus, the output of the MoAE module can be expressed as:

$$y^{\text{MoAE}} = y^{\text{shared}} + \sigma \cdot y^{\text{adaptive}}. \quad (4)$$

The  $\sigma$  factor is zero-initialized so that the visual and text encoders can generate aligned features at the beginning. In practice, we freeze the shared experts and set the adaptive experts to be tunable only. This approach maintains parameter efficiency during mixed training and preserves the multi-modal capabilities of the original model.

We incorporate the MoAE module into the last  $K$  layers of both visual and text encoders, as shown in Figure 3. This strategy makes our method both effective and efficient. The visual feature extraction process can be formulated as:

$$I_i = \mathcal{V}_i(I_{i-1}), \quad i = 1, 2, \dots, L - K$$

$$I_j = \mathcal{V}_j^{\text{MoAE}}(I_{j-1}), \quad j = L - K + 1, \dots, L \quad (5)$$

where  $L$  denotes the number of layers of the visual encoder;  $I_i$  represents the visual features of the  $i$ -th encoder layer; and  $\mathcal{V}^{\text{MoAE}}$  represents the MoAE-equipped visual encoder layer. The text branch operates similarly to the visual branch.

### 3.4. Scene-based differential prompt

To facilitate scene-guided learning, we introduce a **Scene-based Differential Prompt (SDP)** to help the model acquire scene-specific knowledge from different datasets. We utilize 12 datasets spanning 6 image assessment scenarios, including synthetic distortion nature IQA, authentic distortion nature IQA, face IQA, AIGC IQA, underwater



Figure 4. Visual examples from different datasets, which include natural images, underwater images, face images, AI-generated images, and *etc.* The first value is the prediction score and the second value is the ground-truth MOS. Our Gamma can accurately evaluate images from different scenes, demonstrating the generalization and effectiveness. All images are resized for better visibility.

IQA, and IAA, for mixed training. We categorize these datasets into five groups based on their scenes: natural quality, AI-generated quality, underwater quality, face quality, and natural aesthetics. Specifically, for the face quality assessment dataset, we use prompts such as *face bad-quality*, *face poor-quality*, *face fair-quality*, *face good-quality*, *face perfect-quality* appended to the word *image*. For more details on these prompts, please refer to Appendix A.4.

This strategy effectively differentiates the feature space of images from various scenes and enhances scene-specific knowledge, thereby mitigating the MOS bias across different datasets. Experimental results show that this method significantly improves the model’s performance (Table 1).

## 4. Experiments

### 4.1. Datasets

We utilize 12 datasets for unified training and testing, encompassing both image quality and aesthetic assessment tasks. For the IQA task, five different assessment scenarios are included: synthetic distortion nature IQA (SDN-IQA), authentic distortion nature IQA (ADN-IQA), face IQA (F-IQA), AIGC IQA (AG-IQA), and underwater IQA (U-IQA). For the IAA task, we use two classical benchmarks, AVA and AADB. In addition, we use two rare datasets to verify the generalization ability of the model, *i.e.*, exBeDDE and ECIQAD. The exBeDDE is a dehazed image quality assessment (D-IQA) dataset, and the ECIQAD is an enhanced colonoscopy image quality assessment (EC-IQA) dataset. Details about these datasets is provided in Table 9.

### 4.2. Implementation Details

Following the settings in (Su et al., 2020; Ke et al., 2021), we randomly divide each dataset into 80% for training and 20% for testing. The training dataset is a mixture of the training sets of each dataset and we test Gamma on each test data separately. This process is repeated 10 times, and the

median of the 10 scores is reported as the final score. We use the pre-trained weight of UniQA (Zhou et al., 2024b), which uses CLIP-B/16 as multimodal encoder. We freeze the CLIP visual and text encoders, training only the MoAE module and adapter. For the unified training, we train the model for 10 epochs with a batch size of 8. The initial learning rate is set to  $2e-5$ . We normalize the MOS/DMOS scale to  $[0, 1]$  and utilize Adam optimizer (Kingma, 2014) and MSE loss to optimize the model. For the task-specific training, we use different training settings according to the task and size of datasets. More training details are provided in the appendix.

### 4.3. Main Results

Our MoAE-equipped model can be used for task-specific training and mixed training, both of which can achieve state-of-the-art (SOTA) performance, as shown in Table 1.

**Task-specific Training.** We apply our method to 12 image assessment datasets. We use the fixed naive prompt (described in Section 3.2) for training and testing. We observe that our method outperforms all others methods by a significant margin. On some benchmark, our method achieve dramatic improvements, such as SRCC of 0.944 (*v.s.* 0.916) on TID2013 and 0.945 (*v.s.* 0.933) on KonIQ. Since images in these 12 datasets encompass a wide variety of contents and distortion types, it is particularly challenging to consistently achieve the leading performance on all of them.

**Mixed Training.** We conduct mixed training on 12 image assessment datasets. The trained model can be used to assess the images from these datasets. The experimental results are reported in Table 1. When compared with other mixed training models, such as StairIQA and PromptIQA, our method exhibits powerful and superior performance on each dataset. More importantly, our method can also be used to IAA tasks and demonstrates excellent performance. It is worth noting that our mixed training model even achieves results comparable to task-specific models on datasets such

Table 1. Comparison with SOTA task-specific and mixed-training models on 12 datasets for 6 image assessment tasks. ‘‘Gamma’’ and ‘‘Gamma-T’’ denote the mixed-training and task-specific models, respectively. Gamma<sup>†</sup> uses the Scene-based Differential Prompt (SDP) for training and testing. \* indicates that we retrain the model with the same data split as ours.

Task	Synthetic Distortion Nature IQA (SDN-IQA)								Authentic Distortion Nature IQA (ADN-IQA)						
	Dataset	LIVE		CSIQ		TID2013		KADID		LIVEC		KonIQ		SPAQ	
Training Type	Method	SRCC	PLCC	SRCC	PLCC	SRCC	PLCC	SRCC	PLCC	SRCC	PLCC	SRCC	PLCC	SRCC	PLCC
Task Specific	HyperIQA	0.962	0.966	0.923	0.942	0.840	0.858	0.852	0.845	0.859	0.882	0.906	0.917	0.911	0.915
	MUSIQ	0.940	0.911	0.871	0.893	0.773	0.815	0.875	0.872	0.702	0.746	0.916	0.928	0.918	0.921
	TOPIQ	0.943	0.942	0.908	0.925	0.813	0.845	0.877	0.875	0.833	0.868	0.915	0.925	0.914	0.917
	DEIQT	0.980	0.982	0.946	0.963	0.892	0.908	0.889	0.887	0.875	0.894	0.921	0.934	0.919	0.923
	LoDA	0.975	0.979	-	-	0.869	0.901	0.931	0.936	0.876	0.899	0.932	0.944	0.925	0.928
	UniQA	0.981	<b>0.983</b>	0.963	0.973	0.916	0.931	0.940	0.943	0.890	0.905	0.933	0.941	0.924	0.928
Gamma-T	<b>0.982</b>	<b>0.971</b>	<b>0.973</b>	<b>0.978</b>	<b>0.944</b>	<b>0.950</b>	<b>0.960</b>	<b>0.961</b>	<b>0.899</b>	<b>0.921</b>	<b>0.945</b>	<b>0.952</b>	<b>0.928</b>	<b>0.931</b>	
Mixed Training	UNIQUE	0.969	<b>0.968</b>	0.902	0.927	-	-	0.878	0.876	0.854	0.890	0.896	0.901	-	-
	LIQE*	<b>0.972</b>	0.953	0.946	0.943	-	-	0.932	0.933	0.902	0.908	0.920	0.905	-	-
	StairIQA	0.937	0.934	0.768	0.843	0.675	0.773	0.785	0.805	0.780	0.855	0.865	0.896	0.903	0.907
	PromptIQA	0.936	0.934	0.926	0.939	0.903	0.922	0.928	0.931	<b>0.913</b>	<b>0.928</b>	0.929	0.943	0.923	0.926
	Gamma	0.957	0.952	0.949	0.966	0.926	0.934	0.960	0.962	0.851	0.871	<b>0.940</b>	<b>0.949</b>	0.923	0.928
	Gamma <sup>†</sup>	0.953	0.953	<b>0.960</b>	<b>0.968</b>	<b>0.935</b>	<b>0.941</b>	<b>0.962</b>	<b>0.964</b>	0.891	0.914	0.939	<b>0.950</b>	<b>0.929</b>	<b>0.932</b>

Task	Face IQA (F-IQA)			AIGC IQA (AG-IQA)			Underwater IQA (U-IQA)			Image Aesthetic Assessment (IAA)					
	Dataset	GFIQA20k		Dataset	AGIQA3k		Dataset	UWIQA		Dataset	AVA		Dataset	AADB	
Training Type	Method	SRCC	PLCC	Method	SRCC	PLCC	Method	SRCC	PLCC	Method	SRCC	PLCC	Method	SRCC	PLCC
Task Specific	SDD-FIQA	0.602	0.649	DBCNN	0.821	0.876	FDUM	0.694	0.689	MaxViT	0.708	0.745	MUSIQ	0.706	0.712
	IFQA	0.697	0.722	HyperNet	0.836	0.890	UCIQE	0.627	0.626	TANet	0.758	0.765	TANet	0.738	0.737
	TOPIQ	0.966	0.967	CLIPQA	0.843	0.805	URanker	0.674	0.663	VILA	0.774	0.774	TAVAR	0.761	0.763
	GPFIQA	0.964	0.965	PSCR	0.850	0.906	UIQI	0.742	0.741	UniQA	0.776	0.776	UniQA	0.786	0.787
	Gamma-T	<b>0.968</b>	<b>0.968</b>	Ours-T	<b>0.894</b>	<b>0.921</b>	Ours-T	<b>0.870</b>	<b>0.880</b>	Ours-T	<b>0.785</b>	<b>0.784</b>	Ours-T	<b>0.793</b>	<b>0.798</b>
Mixed Training	UNIQUE	-	-	UNIQUE	-	-	UNIQUE	-	-	UNIQUE	-	-	UNIQUE	-	-
	LIQE	-	-	LIQE	-	-	LIQE	-	-	LIQE	-	-	LIQE	-	-
	StairIQA	0.937	0.935	StairIQA	0.755	0.833	StairIQA	0.722	0.727	StairIQA	-	-	StairIQA	-	-
	PromptIQA	<b>0.970</b>	<b>0.971</b>	PromptIQA	0.851	0.901	PromptIQA	<b>0.877</b>	<b>0.884</b>	PromptIQA	-	-	PromptIQA	-	-
	Gamma	<b>0.970</b>	0.970	Gamma	0.870	0.910	Gamma	0.863	0.878	Gamma	0.740	0.737	Gamma	0.742	0.743
	Gamma <sup>†</sup>	<b>0.970</b>	0.970	Gamma <sup>†</sup>	<b>0.887</b>	<b>0.923</b>	Gamma <sup>†</sup>	0.873	<b>0.884</b>	Gamma <sup>†</sup>	<b>0.750</b>	<b>0.749</b>	Gamma <sup>†</sup>	<b>0.756</b>	<b>0.755</b>

Table 2. The effect of Mixture of Assessment Experts (MoAE) and Scene-based Differential Prompt (SDP).

Dataset		LIVEC		KonIQ		LIVE		CSIQ		AGIQA3k		UWIQA		AVA	
MoAE	SDP	SRCC	PLCC	SRCC	PLCC	SRCC	PLCC	SRCC	PLCC	SRCC	PLCC	SRCC	PLCC	SRCC	PLCC
×	×	0.765	0.792	0.858	0.885	0.927	0.918	0.852	0.898	0.800	0.866	0.750	0.768	0.681	0.672
×	✓	0.843	0.856	0.874	0.896	0.929	0.917	0.866	0.901	0.841	0.887	0.770	0.780	0.721	0.715
✓	×	0.851	0.871	0.940	0.949	0.957	0.952	0.949	0.966	0.870	0.910	0.863	0.878	0.740	0.737
✓	✓	0.891	0.914	0.939	0.950	0.960	0.968	0.953	0.953	0.887	0.923	0.873	0.884	0.750	0.749

Table 3. The impact of different number of experts in adaptive experts. We use naive prompt strategy for ablation.

Dataset	LIVEC		CSIQ		TID2013		AGIQA3k		UWIQA	
Experts Number	SRCC	PLCC	SRCC	PLCC	SRCC	PLCC	SRCC	PLCC	SRCC	PLCC
Zero Expert	0.765	0.792	0.852	0.898	0.792	0.826	0.800	0.866	0.750	0.768
One Expert	0.842	0.866	0.945	0.963	0.918	0.931	0.866	0.908	0.859	0.873
Three Experts	0.851	0.871	0.949	0.966	0.926	0.934	0.870	0.910	0.863	0.878
Five Experts	0.854	0.889	0.951	0.965	0.926	0.934	0.872	0.911	0.860	0.876

as KADID, KonIQA, SPAQ, and GFIQA. These results demonstrate that our approach can be effectively applied to different image assessment scenarios.

**Comparison with other mixed training methods.** We conduct a detailed comparison with other mixed training methods, including LIQE, UNIQUE and Q-Align, with the same training datasets. We also perform the cross-dataset

validation with LIQE and UNIQUE. Please refer to Appendix B for details.

**Qualitative Results.** We visualize the image assessment results from different datasets, covering various scenarios, as shown in Figure 4. We can notice that our Gamma can accurately assess images from various tasks. These results shows the high generalization capability of our Gamma.

Table 4. The impact of different model configuration in the proposed MoAE module.

Dataset	LIVEC		CSIQ		AGIQA3k		UWQA		AVA	
	SRCC	PLCC	SRCC	PLCC	SRCC	PLCC	SRCC	PLCC	SRCC	PLCC
Unfreeze shared expert	0.849	0.869	0.946	0.957	0.864	0.904	0.858	0.871	0.720	0.719
w/o Merging factor $\sigma$	0.847	0.866	0.932	0.947	0.851	0.903	0.845	0.869	0.698	0.697
Our MoAE module	0.851	0.871	0.949	0.966	0.870	0.910	0.863	0.878	0.740	0.737

Table 5. The impact of adding MoAE to different numbers of layers for training. Time means training time.

Dataset	Parms	Time	LIVEC		KonIQ		LIVE		CSIQ		AGIQA3k		UWQA		AVA	
			SRCC	PLCC	SRCC	PLCC	SRCC	PLCC	SRCC	PLCC	SRCC	PLCC	SRCC	PLCC	SRCC	PLCC
MoE Layer	Million	Hours														
w/o MoAE	149.9	3.5	0.765	0.792	0.858	0.885	0.927	0.918	0.852	0.898	0.800	0.866	0.750	0.768	0.681	0.672
Last 4 layers	231.8	7.5	0.830	0.859	0.933	0.944	0.954	0.952	0.937	0.960	0.866	0.909	0.853	0.867	0.735	0.732
Last 6 layers	272.7	10.2	0.851	0.871	0.940	0.949	0.957	0.952	0.949	0.966	0.870	0.910	0.863	0.878	0.740	0.737
Last 8 layers	313.6	13.4	0.852	0.883	0.941	0.947	0.956	0.951	0.953	0.967	0.872	0.913	0.866	0.875	0.746	0.743
All 12 layers	395.5	17.2	0.860	0.883	0.939	0.950	0.954	0.950	0.954	0.968	0.881	0.908	0.863	0.868	0.728	0.725

#### 4.4. Ablation Studies

We conduct detailed ablation studies to validate the effectiveness of our proposed modules. Note that we use naive prompt strategy (described in Section 3.2) to perform all ablations unless otherwise specified. We uniformly use 12 datasets for ablation experiments. Considering the page limit, we only show the datasets with relatively large differences in results. More ablations about prompt sensitivity and model efficiency please refer to Appendix C and D.

**Effectiveness of the prompt strategy.** We propose the Scene-based Differential Prompt (SDP) to prompt different datasets. We evaluate the effectiveness of this strategy in Table 1. We can notice that the SDP strategy can improve the model performance on multiple datasets, especially on CSIQ (+1.1% SRCC), LIVEC (+4% SRCC) and AGIQA-3k (+1.7% SRCC). These results demonstrate that the SDP can effectively guide model learn differential features for different datasets, thus enhancing model performance. Furthermore, we ablate the SDP strategy and MOAE module respectively to explore their relationship and impact on model performance. As shown in Table 2, both methods can improve the performance of the model, such as +7.8% SRCC of SDP and +8.6% SRCC of MoAE on LIVEC. This shows the effectiveness of this adaptive expert feature learning and text guidance for multi-dataset learning. When the two methods are used simultaneously, the model can achieve the best results. Therefore, the two methods are mutually beneficial.

**The number of experts.** We explore the impact of different numbers of experts in the adaptive assessment experts. As shown in Table 3 and Figure 5a, the model achieves higher performance with more experts. This suggests that adding experts can better cope with the dataset bias problem when using a mixed training strategy. Using five experts cannot significantly improve the performance as the performance approaches saturation. We use three experts to constitute the adaptive assessment experts in MoAE to achieve the

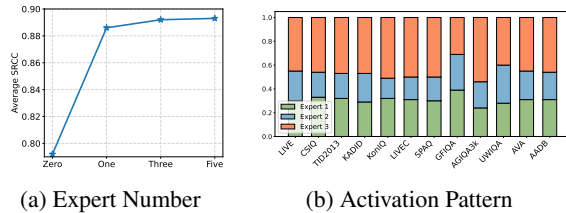


Figure 5. (a) Average performance when using different numbers of experts. Adding adaptive experts significantly improves model performance. (b) Average activations of three experts in the last layer of the visual encoder with naive prompts. Image evaluations of different scenes have different activation patterns.

optimal trade-off between accuracy and efficiency.

**Effect of freezing the shared expert.** We freeze the shared expert in the MoAE to retrain the multimodal capability of original model. This strategy also helps model capture the generalizable and common representation across varying contexts. Table 4 validates this method and shows that it is effective across various datasets.

**Merging features with factor  $\sigma$ .** Table 4 also demonstrates the effect of merging features of shared and adaptive experts with factor  $\sigma$ . We notice that this strategy improves the model performance on different datasets, especially on AVA and AGIQA3k. These results show that it is beneficial to utilize aligned features at the beginning of training and partially using features from adaptive experts.

**Adding adapter to last few layers.** We add the proposed MoAE module into the last few layers of the visual and text encoders. We compare the performance of adding MoAE to different numbers of layers in Table 5. After using MoAE, the performance of the model is significantly improved. We also observe that adding more than six layers of adapters does not improve model performance significantly, but further increases the model parameter and training overhead. Therefore, we integrate MoAE module in the last six layers

Table 6. Results when only one adaptive expert is activated. The weights factors of other experts are set to 0. It can be observed that different experts focus on different datasets.

Dataset	LIVEC		KonIQ		LIVE		CSIQ		AGIQA3k		UWIQA		GFIQA		AVA	
Expert index	SRCC	PLCC	SRCC	PLCC	SRCC	PLCC	SRCC	PLCC	SRCC	PLCC	SRCC	PLCC	SRCC	PLCC	SRCC	PLCC
1-th expert	<b>0.847</b>	<b>0.860</b>	<b>0.927</b>	<b>0.938</b>	<b>0.933</b>	<b>0.933</b>	<b>0.894</b>	<b>0.906</b>	0.815	0.870	<b>0.770</b>	<b>0.779</b>	<b>0.959</b>	<b>0.957</b>	0.666	0.673
2-th expert	0.715	0.672	0.681	0.717	0.900	0.861	0.815	0.846	<b>0.832</b>	<b>0.885</b>	0.755	0.756	0.826	0.797	0.663	0.652
3-th expert	0.768	0.741	0.794	0.818	0.918	0.917	0.833	0.877	0.808	0.910	0.691	0.709	0.903	0.897	<b>0.715</b>	<b>0.716</b>
Gamma	0.851	0.871	0.940	0.949	0.957	0.952	0.949	0.966	0.870	0.910	0.863	0.878	0.970	0.970	0.740	0.737

Table 7. Generalization capability validation on the exBeDDE and ECIQAD datasets. The ‘‘Pretrained weight’’ denotes the model weight of mixed training. We can notice that loading pretrained weight for initialization can improve model performance.

(a) Results on the exBeDDE datasets.				(b) Results on the ECIQAD datasets.			
Method	SRCC	PLCC		Method	SRCC	PLCC	
BRISQUE (Mittal et al., 2012a)	0.890	0.906		BRISQUE (Mittal et al., 2012a)	0.436	0.459	
PSQA-I (Liu et al., 2019)	0.907	0.924		BIQME (Gu et al., 2017)	0.770	0.768	
HyperIQA (Su et al., 2020)	0.917	0.926		BPRI (Min et al., 2017)	0.152	0.181	
FADE (Choi et al., 2015)	0.714	0.729		FRIQUEE (Ghadiyaram & Bovik, 2017)	0.663	0.656	
DHQI (Min et al., 2018)	0.919	0.939		CIQA (Chen et al., 2021)	0.738	0.735	
VDA-DQA (Guan et al., 2022)	0.923	0.942		ECIQ (Ke et al., 2021)	0.839	0.842	
Ours	0.916	0.938		Ours	0.912	0.922	
Ours + Pretrained weight	<b>0.937</b>	<b>0.951</b>		Ours + Pretrained weight	<b>0.917</b>	<b>0.927</b>	

of both visual and text encoder.

**Activation patterns of different datasets.** We visualize the average activation degree of three experts in the last layer of Gamma’s visual encoder for different datasets, as shown in Figure 5b. We can observe that the activation patterns are different for different scenarios. Specifically, the natural image assessment datasets, *e.g.*, LIVE, CSIQ, KADID, show different activation patterns from the face IQA dataset GFIQA and the underwater IQA dataset UWIQA. The synthetic distortion and authentic distortion dataset in nature IQA also have different activation patterns. These indicate that our MoAE module can assign experts with different activation levels to images of different scenarios, thereby capturing the discriminative features effectively.

**Analysis of the adaptive experts.** We add an experiment in which we only use one adaptive expert and set the router weights of the other experts to 0, to explore the preferences of different experts for different datasets. As shown in Table 6, the first expert performs well on most datasets, indicating it learns a general image assessment ability. The second and third experts focus on AIGC IQA and IAA tasks, respectively, and the third expert also shows excellent evaluation capabilities for natural images. These results indicate that different experts have learned domain-specific features of different datasets. They collaborate to achieve the powerful image assessment model Gamma.

#### 4.5. Generalization Capability Validation

We further validate the generalization capability of our method on two datasets, exBeDDE and ECIQAD. The

exBeDDE is a dehazed IQA dataset and the ECIQAD is an enhanced colonoscopy IQA dataset, which belong to completely different evaluation domains compared to the used datasets in mixed training. We use naive prompt strategy for training and testing. The experimental results are reported in Table 7. We notice that our method can achieve competitive performance on these two datasets, showing the effectiveness and generalization capability of our method. More importantly, when we load the pretrained weight of Gamma for initialization, the performance of both datasets is improved and our method achieves the SOTA results. This indicates that our pretrained Gamma can be an effective foundation model to aid other assessment fields.

## 5. Conclusion

This paper introduces Gamma, a generic image assessment model that can be applied to various image scenarios. To achieve this, we utilize the mixed training of different datasets to obtain the assessment abilities of different scenarios. We propose a Mixture of Assessment Expert (MoAE) module and a Scene-based Differential Prompt (SDP) strategy to effectively cope with the MOS bias in different datasets. MoAE utilizes shared experts and adaptive experts to extract common and representative features adaptively. SDP strategy employs different prompts for different datasets to provide guidance for feature learning. Extensive experiments demonstrate that our method can achieve SOTA performance on various datasets simultaneously, showing the strong generalization and general image assessment capabilities.



## Impact Statement

This paper presents work whose goal is to advance the field of Machine Learning. There are many potential societal consequences of our work, none which we feel must be specifically highlighted here.

## References

- Chen, C., Mo, J., Hou, J., Wu, H., Liao, L., Sun, W., Yan, Q., and Lin, W. Topiq: A top-down approach from semantics to distortions for image quality assessment. *IEEE Transactions on Image Processing*, 2024a.
- Chen, H., Chai, X., Shao, F., Wang, X., Jiang, Q., Meng, X., and Ho, Y.-S. Perceptual quality assessment of cartoon images. *IEEE Transactions on Multimedia*, 25:140–153, 2021.
- Chen, T., Chen, X., Du, X., Rashwan, A., Yang, F., Chen, H., Wang, Z., and Li, Y. Adamv-moe: Adaptive multi-task vision mixture-of-experts. In *Proceedings of the IEEE/CVF International Conference on Computer Vision*, pp. 17346–17357, 2023.
- Chen, Z., Qin, H., Wang, J., Yuan, C., Li, B., Hu, W., and Wang, L. Promptiqa: Boosting the performance and generalization for no-reference image quality assessment via prompts. *arXiv preprint arXiv:2403.04993*, 2024b.
- Choi, L. K., You, J., and Bovik, A. C. Referenceless prediction of perceptual fog density and perceptual image defogging. *IEEE Transactions on Image Processing*, 24(11):3888–3901, 2015.
- Dai, D., Deng, C., Zhao, C., Xu, R., Gao, H., Chen, D., Li, J., Zeng, W., Yu, X., Wu, Y., et al. Deepseekmoe: Towards ultimate expert specialization in mixture-of-experts language models. *arXiv preprint arXiv:2401.06066*, 2024.
- Dai, Y., Li, X., Liu, J., Tong, Z., and Duan, L.-Y. Generalizable person re-identification with relevance-aware mixture of experts. In *Proceedings of the IEEE/CVF conference on computer vision and pattern recognition*, pp. 16145–16154, 2021.
- Fang, Y., Zhu, H., Zeng, Y., Ma, K., and Wang, Z. Perceptual quality assessment of smartphone photography. In *CVPR*, pp. 3677–3686, 2020.
- Feng, Z., Zhang, Z., Yu, X., Fang, Y., Li, L., Chen, X., Lu, Y., Liu, J., Yin, W., Feng, S., et al. Ernie-vilg 2.0: Improving text-to-image diffusion model with knowledge-enhanced mixture-of-denoising-experts. In *Proceedings of the IEEE/CVF Conference on Computer Vision and Pattern Recognition*, pp. 10135–10145, 2023.
- Ghadiyaram, D. and Bovik, A. C. Massive online crowd-sourced study of subjective and objective picture quality. *IEEE TIP*, 25(1):372–387, 2015.
- Ghadiyaram, D. and Bovik, A. C. Perceptual quality prediction on authentically distorted images using a bag of features approach. *Journal of vision*, 17(1):32–32, 2017.
- Gu, K., Tao, D., Qiao, J.-F., and Lin, W. Learning a no-reference quality assessment model of enhanced images with big data. *IEEE transactions on neural networks and learning systems*, 29(4):1301–1313, 2017.
- Guan, T., Li, C., Gu, K., Liu, H., Zheng, Y., and Wu, X.-j. Visibility and distortion measurement for no-reference dehazed image quality assessment via complex contourlet transform. *IEEE Transactions on Multimedia*, 25:3934–3949, 2022.
- Guo, C., Wu, R., Jin, X., Han, L., Zhang, W., Chai, Z., and Li, C. Underwater ranker: Learn which is better and how to be better. In *Proceedings of the AAAI conference on artificial intelligence*, volume 37, pp. 702–709, 2023.
- He, S., Zhang, Y., Xie, R., Jiang, D., and Ming, A. Rethinking image aesthetics assessment: Models, datasets and benchmarks. In *IJCAI*, pp. 942–948, 2022.
- Hosu, V., Goldlucke, B., and Saupe, D. Effective aesthetics prediction with multi-level spatially pooled features. In *proceedings of the IEEE/CVF conference on computer vision and pattern recognition*, pp. 9375–9383, 2019.
- Hosu, V., Lin, H., Sziranyi, T., and Saupe, D. Koniq-10k: An ecologically valid database for deep learning of blind image quality assessment. *IEEE TIP*, 29:4041–4056, 2020.
- Jo, B., Cho, D., Park, I. K., and Hong, S. Ifqa: interpretable face quality assessment. In *Proceedings of the IEEE/CVF winter conference on applications of computer vision*, pp. 3444–3453, 2023.
- Ke, J., Wang, Q., Wang, Y., Milanfar, P., and Yang, F. Musiq: Multi-scale image quality transformer. In *Proceedings of the IEEE/CVF international conference on computer vision*, pp. 5148–5157, 2021.
- Ke, J., Ye, K., Yu, J., Wu, Y., Milanfar, P., and Yang, F. Vila: Learning image aesthetics from user comments with vision-language pretraining. In *Proceedings of the IEEE/CVF Conference on Computer Vision and Pattern Recognition*, pp. 10041–10051, 2023.
- Kingma, D. P. Adam: A method for stochastic optimization. *arXiv preprint arXiv:1412.6980*, 2014.

- Kong, S., Shen, X., Lin, Z., Mech, R., and Fowlkes, C. Photo aesthetics ranking network with attributes and content adaptation. In *ECCV*, pp. 662–679. Springer, 2016.
- Langley, P. Crafting papers on machine learning. In Langley, P. (ed.), *Proceedings of the 17th International Conference on Machine Learning (ICML 2000)*, pp. 1207–1216, Stanford, CA, 2000. Morgan Kaufmann.
- Larson, E. C. and Chandler, D. M. Most apparent distortion: full-reference image quality assessment and the role of strategy. *Journal of electronic imaging*, 19(1):011006–011006, 2010.
- Li, C., Zhang, Z., Wu, H., Sun, W., Min, X., Liu, X., Zhai, G., and Lin, W. Agiqa-3k: An open database for ai-generated image quality assessment. *IEEE Transactions on Circuits and Systems for Video Technology*, 2023a.
- Li, D., Jiang, T., Lin, W., and Jiang, M. Which has better visual quality: The clear blue sky or a blurry animal? *IEEE Transactions on Multimedia*, 21(5):1221–1234, 2018.
- Li, L., Huang, Y., Wu, J., Yang, Y., Li, Y., Guo, Y., and Shi, G. Theme-aware visual attribute reasoning for image aesthetics assessment. *IEEE Transactions on Circuits and Systems for Video Technology*, 33(9):4798–4811, 2023b.
- Liang, Y., He, J., Li, G., Li, P., Klimovskiy, A., Carolan, N., Sun, J., Pont-Tuset, J., Young, S., Yang, F., et al. Rich human feedback for text-to-image generation. In *Proceedings of the IEEE/CVF Conference on Computer Vision and Pattern Recognition*, pp. 19401–19411, 2024.
- Lin, H., Hosu, V., and Saupé, D. Kadid-10k: A large-scale artificially distorted iqa database. In *2019 Eleventh International Conference on Quality of Multimedia Experience (QoMEX)*, pp. 1–3. IEEE, 2019.
- Liu, L., Wang, T., and Huang, H. Pre-attention and spatial dependency driven no-reference image quality assessment. *IEEE Transactions on Multimedia*, 21(9):2305–2318, 2019.
- Liu, Q., Wu, X., Zhao, X., Zhu, Y., Xu, D., Tian, F., and Zheng, Y. When moe meets llms: Parameter efficient fine-tuning for multi-task medical applications. In *Proceedings of the 47th International ACM SIGIR Conference on Research and Development in Information Retrieval*, pp. 1104–1114, 2024.
- Liu, Y., Gu, K., Cao, J., Wang, S., Zhai, G., Dong, J., and Kwong, S. Uiqi: A comprehensive quality evaluation index for underwater images. *IEEE Transactions on Multimedia*, 2023.
- Min, X., Gu, K., Zhai, G., Liu, J., Yang, X., and Chen, C. W. Blind quality assessment based on pseudo-reference image. *IEEE Transactions on Multimedia*, 20(8):2049–2062, 2017.
- Min, X., Zhai, G., Gu, K., Yang, X., and Guan, X. Objective quality evaluation of dehazed images. *IEEE Transactions on Intelligent Transportation Systems*, 20(8):2879–2892, 2018.
- Mittal, A., Moorthy, A. K., and Bovik, A. C. No-reference image quality assessment in the spatial domain. *IEEE Transactions on image processing*, 21(12):4695–4708, 2012a.
- Mittal, A., Soundararajan, R., and Bovik, A. C. Making a “completely blind” image quality analyzer. *IEEE Signal processing letters*, 20(3):209–212, 2012b.
- Murray, N., Marchesotti, L., and Perronnin, F. Ava: A large-scale database for aesthetic visual analysis. In *CVPR*, pp. 2408–2415. IEEE, 2012.
- Ou, F.-Z., Chen, X., Zhang, R., Huang, Y., Li, S., Li, J., Li, Y., Cao, L., and Wang, Y.-G. Sdd-fiq: Unsupervised face image quality assessment with similarity distribution distance. In *Proceedings of the IEEE/CVF conference on computer vision and pattern recognition*, pp. 7670–7679, 2021.
- Ponomarenko, N., Ieremeiev, O., Lukin, V., Egiazarian, K., Jin, L., Astola, J., Vozel, B., Chehdi, K., Carli, M., Battisti, F., et al. Color image database tid2013: Peculiarities and preliminary results. In *European workshop on visual information processing (EUVIP)*, pp. 106–111. IEEE, 2013.
- Qin, G., Hu, R., Liu, Y., Zheng, X., Liu, H., Li, X., and Zhang, Y. Data-efficient image quality assessment with attention-panel decoder. In *Proceedings of the AAAI Conference on Artificial Intelligence*, volume 37, pp. 2091–2100, 2023.
- Radford, A., Kim, J. W., Hallacy, C., Ramesh, A., Goh, G., Agarwal, S., Sastry, G., Askell, A., Mishkin, P., Clark, J., et al. Learning transferable visual models from natural language supervision. In *International conference on machine learning*, pp. 8748–8763. PMLR, 2021.
- Riquelme, C., Puigcerver, J., Mustafa, B., Neumann, M., Jenatton, R., Susano Pinto, A., Keysers, D., and Houlsby, N. Scaling vision with sparse mixture of experts. *Advances in Neural Information Processing Systems*, 34: 8583–8595, 2021.
- Rombach, R., Blattmann, A., Lorenz, D., Esser, P., and Ommer, B. High-resolution image synthesis with latent

- diffusion models. In *Proceedings of the IEEE/CVF conference on computer vision and pattern recognition*, pp. 10684–10695, 2022.
- Shazeer, N., Mirhoseini, A., Maziarz, K., Davis, A., Le, Q., Hinton, G., and Dean, J. Outrageously large neural networks: The sparsely-gated mixture-of-experts layer. *arXiv preprint arXiv:1701.06538*, 2017.
- Sheikh, H. R., Sabir, M. F., and Bovik, A. C. A statistical evaluation of recent full reference image quality assessment algorithms. *IEEE TIP*, 15(11):3440–3451, 2006.
- Su, S., Yan, Q., Zhu, Y., Zhang, C., Ge, X., Sun, J., and Zhang, Y. Blindly assess image quality in the wild guided by a self-adaptive hyper network. In *Proceedings of the IEEE/CVF conference on computer vision and pattern recognition*, pp. 3667–3676, 2020.
- Su, S., Lin, H., Hosu, V., Wiedemann, O., Sun, J., Zhu, Y., Liu, H., Zhang, Y., and Saupe, D. Going the extra mile in face image quality assessment: A novel database and model. *IEEE TMM*, 2023a.
- Su, S., Lin, H., Hosu, V., Wiedemann, O., Sun, J., Zhu, Y., Liu, H., Zhang, Y., and Saupe, D. Going the extra mile in face image quality assessment: A novel database and model. *IEEE Transactions on Multimedia*, 2023b.
- Sun, W., Min, X., Tu, D., Ma, S., and Zhai, G. Blind quality assessment for in-the-wild images via hierarchical feature fusion and iterative mixed database training. *IEEE Journal of Selected Topics in Signal Processing*, 17(6): 1178–1192, 2023.
- Talebi, H. and Milanfar, P. Nima: Neural image assessment. *IEEE transactions on image processing*, 27(8): 3998–4011, 2018.
- Tang, L., Tian, Z., Li, K., He, C., Zhou, H., Zhao, H., Li, X., and Jia, J. Mind the interference: Retaining pre-trained knowledge in parameter efficient continual learning of vision-language models. In *European Conference on Computer Vision*, pp. 346–365. Springer, 2024.
- Tu, Z., Talebi, H., Zhang, H., Yang, F., Milanfar, P., Bovik, A., and Li, Y. Maxvit: Multi-axis vision transformer. In *European conference on computer vision*, pp. 459–479. Springer, 2022.
- Wang, J., Chan, K. C., and Loy, C. C. Exploring clip for assessing the look and feel of images. In *Proceedings of the AAAI Conference on Artificial Intelligence*, volume 37, pp. 2555–2563, 2023.
- Wang, W., Bao, H., Dong, L., Bjorck, J., Peng, Z., Liu, Q., Aggarwal, K., Mohammed, O. K., Singhal, S., Som, S., et al. Image as a foreign language: Beit pretraining for all vision and vision-language tasks. *arXiv preprint arXiv:2208.10442*, 2022.
- Wu, H., Zhang, Z., Zhang, W., Chen, C., Liao, L., Li, C., Gao, Y., Wang, A., Zhang, E., Sun, W., et al. Q-align: Teaching llms for visual scoring via discrete text-defined levels. *arXiv preprint arXiv:2312.17090*, 2023.
- Xiao, Y., Ma, Y., Li, S., Zhou, H., Liao, R., and Li, X. Semanticac: semantics-assisted framework for audio classification. In *ICASSP 2023-2023 IEEE International Conference on Acoustics, Speech and Signal Processing (ICASSP)*, pp. 1–5. IEEE, 2023.
- Xiao, Y., Luo, Z., Liu, Y., Ma, Y., Bian, H., Ji, Y., Yang, Y., and Li, X. Bridging the gap: A unified video comprehension framework for moment retrieval and highlight detection. In *Proceedings of the IEEE/CVF Conference on Computer Vision and Pattern Recognition*, pp. 18709–18719, 2024.
- Xu, K., Liao, L., Xiao, J., Chen, C., Wu, H., Yan, Q., and Lin, W. Boosting image quality assessment through efficient transformer adaptation with local feature enhancement. In *Proceedings of the IEEE/CVF Conference on Computer Vision and Pattern Recognition*, pp. 2662–2672, 2024.
- Yang, M. and Sowmya, A. An underwater color image quality evaluation metric. *IEEE Transactions on Image Processing*, 24(12):6062–6071, 2015.
- Yang, N., Zhong, Q., Li, K., Cong, R., Zhao, Y., and Kwong, S. A reference-free underwater image quality assessment metric in frequency domain. *Signal Processing: Image Communication*, 94:116218, 2021a.
- Yang, N., Zhong, Q., Li, K., Cong, R., Zhao, Y., and Kwong, S. A reference-free underwater image quality assessment metric in frequency domain. *Signal Processing: Image Communication*, 94:116218, 2021b.
- Yang, R., Song, L., Li, Y., Zhao, S., Ge, Y., Li, X., and Shan, Y. Gpt4tools: Teaching large language model to use tools via self-instruction. *Advances in Neural Information Processing Systems*, 36, 2024.
- Ying, Z., Niu, H., Gupta, P., Mahajan, D., Ghadiyaram, D., and Bovik, A. From patches to pictures (paq-2-piq): Mapping the perceptual space of picture quality. In *CVPR*, pp. 3575–3585, 2020.
- You, Z., Li, Z., Gu, J., Yin, Z., Xue, T., and Dong, C. Depicting beyond scores: Advancing image quality assessment through multi-modal language models. *arXiv preprint arXiv:2312.08962*, 2023.

- Yuan, J., Cao, X., Cao, L., Lin, J., and Cao, X. Pscr: Patches sampling-based contrastive regression for aigc image quality assessment. *arXiv preprint arXiv:2312.05897*, 2023.
- Yue, G., Cheng, D., Zhou, T., Hou, J., Liu, W., Xu, L., Wang, T., and Cheng, J. Perceptual quality assessment of enhanced colonoscopy images: A benchmark dataset and an objective method. *IEEE Transactions on Circuits and Systems for Video Technology*, 33(10):5549–5561, 2023.
- Zhang, W., Ma, K., Yan, J., Deng, D., and Wang, Z. Blind image quality assessment using a deep bilinear convolutional neural network. *IEEE TCSVT*, 30(1):36–47, 2018.
- Zhang, W., Ma, K., Zhai, G., and Yang, X. Uncertainty-aware blind image quality assessment in the laboratory and wild. *IEEE Transactions on Image Processing*, 30: 3474–3486, 2021.
- Zhang, W., Zhai, G., Wei, Y., Yang, X., and Ma, K. Blind image quality assessment via vision-language correspondence: A multitask learning perspective. In *Proceedings of the IEEE/CVF conference on computer vision and pattern recognition*, pp. 14071–14081, 2023.
- Zhao, S., Zhang, L., Huang, S., Shen, Y., and Zhao, S. Dehazing evaluation: Real-world benchmark datasets, criteria, and baselines. *IEEE Transactions on Image Processing*, 29:6947–6962, 2020.
- Zhao, S., Zhang, L., Shen, Y., and Zhou, Y. Refinednet: A weakly supervised refinement framework for single image dehazing. *IEEE Transactions on Image Processing*, 30: 3391–3404, 2021.
- Zhou, H., Yang, R., Hu, R., Shu, C., Tang, X., and Li, X. Etdnet: Efficient transformer-based detection network for surface defect detection. *IEEE transactions on instrumentation and measurement*, 72:1–14, 2023.
- Zhou, H., Hu, R., and Li, X. Video object segmentation with dynamic query modulation. In *2024 IEEE International Conference on Multimedia and Expo (ICME)*, pp. 1–6. IEEE, 2024a.
- Zhou, H., Tang, L., Yang, R., Qin, G., Zhang, Y., Hu, R., and Li, X. Uniqqa: Unified vision-language pre-training for image quality and aesthetic assessment. *arXiv preprint arXiv:2406.01069*, 2024b.
- Zhou, H., Yang, R., Zhang, Y., Duan, H., Huang, Y., Hu, R., Li, X., and Zheng, Y. Unihead: unifying multi-perception for detection heads. *IEEE Transactions on Neural Networks and Learning Systems*, 2024c.

## A. More Implementation Details

### A.1. Evaluation Criteria

We use Spearman’s Rank-Order Correlation Coefficient (SRCC) and Pearson’s Linear Correlation Coefficient (PLCC) as criteria to measure the performance of IQA models. Both coefficients range from 0 to 1, with higher values indicating better performance.

### A.2. Training Details

We follow the typical training strategy to fine-tune each dataset, including random cropping and random horizontal flipping. We conduct all experiments on 3090 GPU. Mixed training of the 12 datasets takes 10 hours on a 3090 GPU. For the task-specific training, Table 8 shows the detailed training setting for the different datasets. We use the learning rate of  $2e-5$  for all datasets.

Table 8. Training settings for different datasets.

Dataset	Task	Epoch	Batch size
LIVE (Sheikh et al., 2006)	SDN-IQA	50	8
CSIQ (Larson & Chandler, 2010)	SDN-IQA	50	8
TID2013 (Ponomarenko et al., 2013)	SDN-IQA	20	8
KADID (Lin et al., 2019)	SDN-IQA	20	8
CLIVE (Ghadiyaram & Bovik, 2015)	ADN-IQA	50	8
KonIQ (Hosu et al., 2020)	ADN-IQA	20	8
SPAQ (Fang et al., 2020)	ADN-IQA	20	8
GFIQA20k (Su et al., 2023b)	F-IQA	10	8
AGIQA3k (Li et al., 2023a)	AG-IQA	20	8
UWIQA (Yang et al., 2021a)	U-IQA	50	8
AVA (Murray et al., 2012)	IAA	20	128
AADB (Kong et al., 2016)	IAA	20	8
exBeDDE (Zhao et al., 2020)	D-IQA	20	8
ECIQAD (Yue et al., 2023)	EC-IQA	20	8

### A.3. Datasets

In this paper, we use a total of 14 datasets, 12 of which are used for unified training and 2 are used to evaluate the generalization ability of our model. We present the details of the used datasets in Table 9.

### A.4. Details of the Scene-based Differential Prompt

In the Scene-based Differential Prompt, we use different prompts for datasets from different scene. Specifically, we divide datasets into five categories, *i.e.*, natural IQA, AI-generated IQA, underwater IQA, face IQA, natural IAA. We present the details in Table 11.

## B. Comparison with other mixed training methods

In this subsection, we conduct a more detailed comparison with other mixed training methods. We first compare with LIQE and UNIQUE using the same training data and data splitting ratios. As shown in Table 12, our method achieves better performance on most datasets than LIQE and UNIQUE, especially on the KADID (+2.5% SRCC) and BID (+2.6% SRCC) datasets compared with LIQE. On other datasets, *i.e.*, LIVE and LIVEC, our model also achieves competitive results. Overall, our model has superior performance on these five datasets.

In addition, we conduct cross dataset validation under this setting. As shown in Table 13, our method achieves highly competitive results on TID2013 and SPAQ, demonstrating the strong generalization capability of our method. Note that using mix-training of more dataset can significantly enhance the zero-shot performance on other datasets, *i.e.*, 0.770 SRCC to 0.818 SRCC on AIGC2023 dataset, demonstrating the effectiveness of mix-training via MoAE and SDP methods.

Compared with Q-Align, as shown in Table 14, our method achieves better results on KonIQ and KADID, and is also highly competitive on SPAQ.

Table 9. Detail information about the 14 used datasets.

Dataset	Task	Image Number	Label Type	Range
LIVE (Sheikh et al., 2006)	SDN-IQA	779	DMOS	[1, 100]
CSIQ (Larson & Chandler, 2010)		866	DMOS	[0, 1]
TID2013 (Ponomarenko et al., 2013)		3,000	MOS	[0, 9]
KADID-10k (Lin et al., 2019)		10,125	MOS	[1, 5]
SPAQ (Fang et al., 2020)	ADN-IQA	11,125	MOS	[0, 100]
LIVEC (Ghadiyaram & Bovik, 2015)		1,162	MOS	[1, 100]
KonIQ-10K (Hosu et al., 2020)		10,073	MOS	[0, 100]
GFIQA20k (Su et al., 2023a)	F-IQA	19,988	MOS	[0, 1]
AGIQA3k (Li et al., 2023a)	AG-IQA	2,982	MOS	[0, 1]
UWIQA (Yang et al., 2021a)	U-IQA	890	MOS	[0, 1]
AVA (Murray et al., 2012)	IAA	250,000	MOS	[0, 10]
AADB (Kong et al., 2016)	IAA	10,000	MOS	[0, 1]
exBeDDE (Zhao et al., 2020)	D-IQA	1670	MOS	[0, 1]
ECIQAD (Yue et al., 2023)	EC-IQA	2400	MOS	[1, 9]

Table 10. Detail information about the 14 used datasets.

Method	Trainable Params	FLOPs	Inference time	KonIQ SRCC	KADID SRCC
Q-Align (Wu et al., 2023)	8.2B (8200M)	-	0.1s	0.938	0.934
LIQE (Zhang et al., 2023)	151M	17.40G	0.02s	0.919	0.930
Gamma	122.8M	28.45G	0.025s	<b>0.939</b>	<b>0.962</b>

### C. Sensitivity analysis of prompt

We analyze the sensitivity of prompts when the model is trained with scene-based differential prompts (SDP). Table 15 shows that using prompts different from SDP slightly reduces performance on most datasets, showing the robustness of our method. The quality prompt performs better than the general prompt on the IQA task, but performs worse on the IAA task, indicating the importance of appropriate prompts. In conclusion, our method is robust and insensitive to prompts, nevertheless we suggest using correct prompts to obtain better performance.

### D. Model efficiency analysis

We calculate the number of parameters, computation, and inference time of our model. For inference time, we use a  $224 \times 224$  image for testing. All indicators are obtained on a 3090 GPU. We compare it with two classic mixed training methods, LIQE (Zhang et al., 2023) and Q-Align (Wu et al., 2023). As shown in Table 10, our model achieves the best accuracy and efficiency. Compared with LIQE, our model has significantly better performance. Compared with Q-Align, we not only have better performance, but also have significantly lower model parameters and inference latency.

Table 11. Text prompts used in Scene-based Differential Prompt.

Dataset	Prompt
LIVE, CSIQ, TID2013, KADID LIVEC, KonIQ, SPAQ	{natural bad-quality image, natural poor-quality image, natural fair-quality image, natural good-quality image, natural perfect-quality image}
AGIQA3k	{AI-generated bad-quality image, AI-generated poor-quality image, AI-generated fair-quality image, AI-generated good-quality image, AI-generated perfect-quality image}
GFIQA20k	{face bad-quality image, face poor-quality image, face fair-quality image, face good-quality image, face perfect-quality image}
UWIQA	{underwater bad-quality image, underwater poor-quality image, underwater fair-quality image, underwater good-quality image, underwater perfect-quality image}
AVA, AADB	{natural bad-aesthetics image, natural poor-aesthetics image, natural fair-aesthetics image, natural good-aesthetics image, natural perfect-aesthetics image}

Table 12. Comparison with LIQE (Zhang et al., 2023) and UNIQUE (Zhang et al., 2021) when using the same training data.

Dataset	LIVE		CSIQ		KADID		BID		LIVEC		KonIQ		Average	
Method	SRCC	PLCC	SRCC	PLCC	SRCC	PLCC	SRCC	PLCC	SRCC	PLCC	SRCC	PLCC	SRCC	PLCC
UNIQUE	0.961	0.952	0.902	0.921	0.884	0.885	0.852	0.875	0.854	0.884	0.895	0.900	0.891	0.903
LIQE	0.970	0.951	0.936	0.939	0.930	0.931	0.875	0.900	0.904	0.910	0.919	0.908	0.922	0.923
Gamma <sup>†</sup>	0.960	0.947	0.936	0.957	0.955	0.956	0.901	0.925	0.890	0.915	0.933	0.946	<b>0.929</b>	<b>0.941</b>

Table 13. Cross-dataset validation when using the same training data as LIQE and UNIQUE. The subscripts “s” and “r” stand for models trained on KADID and KonIQ, respectively. Gamma<sup>†</sup> uses the same 6 datasets as LIQE and UNIQUE for training and validation. Gamma<sup>††</sup> uses 12 datasets (include TID2012 and SPAQ) for training and performs zero-shot cross dataset validation on other datasets. Gamma<sup>††</sup> significantly enhances the zero-shot performance on other datasets, showing the effectiveness of mix-training via MoAE and SDP methods.

Dataset	TID2013	SPAQ	AIGC2023	Average
NIQE	0.314	0.578	-	0.446
DBCNN <sub>s</sub>	0.686	0.412	0.730	0.609
PaQ2PiQ	0.423	0.823	0.643	0.630
MUSIQ <sub>r</sub>	0.584	0.853	0.736	0.724
UNIQUE	0.768	0.838	0.761	0.789
LIQE	0.811	0.881	0.744	0.812
Gamma <sup>†</sup>	0.805	0.894	0.770	<b>0.823</b>
Gamma <sup>††</sup>	-	-	0.818	-

Table 14. Comparison with Q-Align (Wu et al., 2023) when using the same training data.

Dataset	KonIQ		SPAQ		KADID		Average	
Method	SRCC	PLCC	SRCC	PLCC	SRCC	PLCC	SRCC	PLCC
Q-Align	0.938	0.945	0.931	0.933	0.934	0.935	0.934	0.938
Gamma <sup>†</sup>	0.940	0.950	0.928	0.932	0.962	0.964	<b>0.943</b>	<b>0.949</b>

Table 15. Sensitivity analysis of prompt. Quality prompt is {bad-quality, poor-quality, fair-quality, good-quality, perfect-quality}; General prompt replaces the scene prompt (see Table 11) to “general”, e.g., {underwear bad-quality image} to {general bad-quality image}.

Dataset	LIVEC		KonIQ		LIVE		CSIQ		AGIQA3k		UWIQA		AVA	
Prompt	SRCC	PLCC	SRCC	PLCC	SRCC	PLCC	SRCC	PLCC	SRCC	PLCC	SRCC	PLCC	SRCC	PLCC
General prompt	0.882	0.888	0.921	0.920	0.943	0.930	0.948	0.957	0.775	0.843	0.832	0.842	0.648	0.624
Quality prompt	0.885	0.889	0.931	0.940	0.950	0.946	0.946	0.951	0.822	0.872	0.861	0.876	0.451	0.455
SDP	0.891	0.914	0.939	0.950	0.953	0.953	0.960	0.968	0.887	0.923	0.873	0.884	0.750	0.749